Tectonophysics, 108 (1984) 93–134
Elsevier Science Publishers B.V., Amsterdam – Printed in The Netherlands

A SEISMIC HAZARD MAP OF INDIA AND ADJACENT AREAS

K.N. KHATTRI [1], A.M. ROGERS [2], D.M. PERKINS [2] and S.T. ALGERMISSEN [2]

[1] *Earth Science Department, Roorkee University, Roorkee, U.P. 247672 (India)*
[2] *United States Geological Survey, MS 966, Box 25046, Denver Federal Center, Denver, CO 80225 (U.S.A.)*

(Received December 28, 1982; revised version accepted February 22, 1984)

ABSTRACT

Khattri, K.N., Rogers, A.M., Perkins, D.M. and Algermissen, S.T., 1984. A seismic hazard map of India and adjacent areas. *Tectonophysics*, 108: 93–134.

We have produced a probabilistic seismic hazard map showing peak ground accelerations in rock for India and neighboring areas having a 10% probability of being exceeded in 50 years. Seismogenic zones were identified on the basis of historical seismicity, seismotectonics and geology of the region. Procedures for reducing the incompleteness of earthquake catalogs were followed before estimating recurrence parameters. An eastern United States acceleration attenuation relationship was employed after it was found that intensity attenuation for the Indian region and the eastern United States was similar. The largest probabilistic accelerations are obtained in the seismotectonic belts of Kirthar, Hindukush, Himalaya, Arakan-Yoma, and the Shillong massif where values of over 70% g have been calculated.

INTRODUCTION

Many parts of the Indian subcontinent have historically high seismicity. Figure 1 shows all the epicenters of the historical shallow ($h < 70$ km) earthquakes in the region and Fig. 2 illustrates epicenters of the intermediate-depth events. Seven catastrophic earthquakes of magnitude greater than 8 have occurred in the western, northern, and eastern parts of India and adjacent countries in the past 80 years. Peninsular India, by contrast, is relatively aseismic, having had only infrequent earthquakes of moderate intensity. The main seismogenic belts are associated with the collision plate boundary between the Indian and the Eurasian plates which is marked by the Kirthar Sulaiman, Himalaya and Arakan-Yoma mountain ranges.

Scientists of the Geological Survey of India were among the first to study the destructive effects of earthquakes (e.g., Oldham, 1899), and it was recognized early that potential seismic hazards should be considered in the development of urban centers located within areas of high seismicity. Various seismic hazard maps which have been produced for the Indian region can be classified into two categories. The

0040-1951/84/$03.00

first category consists of those maps that assign seismic hazard to zones without attaching any probabilities to the ground-motion parameter (Auden, 1959; Tandon, 1956; West, 1937; Krishna, 1959; Mithal and Srivastava, 1959; Guha, 1962; Gubin, 1968; Gaur and Chouhan, 1968; ISI, 1975 and Srivastava, 1976; Kaila et al., 1972, Kaila and Rao, 1979). The second category consists of probabilistic hazard maps (Basu and Nigam, 1977, 1978; Sinvhal et al., 1976; Khattri et al., 1978; Hattori, 1979; and Basu and Srivastava, 1981).

A general drawback of the hazard map belonging to the first category is that heavy emphasis is placed on the sites of the past great earthquakes without generalization for the underlying geodynamic process. Sites of past great earthquakes have been encircled by contours showing highest seismic hazard. If great earthquakes, however, eventually fill all parts of the plate boundary, areas considered as having low seismic hazard on the first type of map will be found to be in error.

In addition to identifying areas subject to earthquake damage, however, additional information is required for designing modern, major structures in seismic areas. In order to economically provide suitable earthquake resistance to civil works, it is important to estimate the likelihood with which certain specified ground-motion parameters (e.g., intensity, peak acceleration, etc.) will be exceeded or, alternatively, the probability with which they will not be exceeded in a given time.

Maps in the second catagory incorporate statistical models of the earthquake process (Cornell, 1968; Algermissen and Perkins, 1976). These procedures combine information about earthquake occurrence in time and space, based both on geological and historical data, and attenuation of ground-motion intensity with source–site distance, to provide probabilistic statements about the seismic hazard at a location. Although probabilistic maps have been produced for this region or subregions before, this paper seeks to improve upon previously published seismic zoning maps of India and adjacent areas by taking into consideration the following aspects:

(1) Identification of seismic source zones that have the same generalized geological features and similar seismogenic processes.

(2) Computation of frequency–magnitude relations for the source regions using data with the longest possible time base and correcting the data in each magnitude interval for incompleteness using the procedures developed by Stepp (1973).

(3) Modelling earthquakes as line rupture sources along fault lineaments in the source zones.

(4) Use of an appropriate acceleration–attenuation function for the Indian region.

(5) Taking into account the hazard due to intermediate-depth earthquakes.

For the purpose of statistical analysis in this study, an earthquake catalogue was assembled and partitioned into subsets corresponding to source zones. The subsets of reported earthquakes for each source zone were further subdivided into two classes: (1) shallow focus earthquakes with depths less than 70 km, and (2)

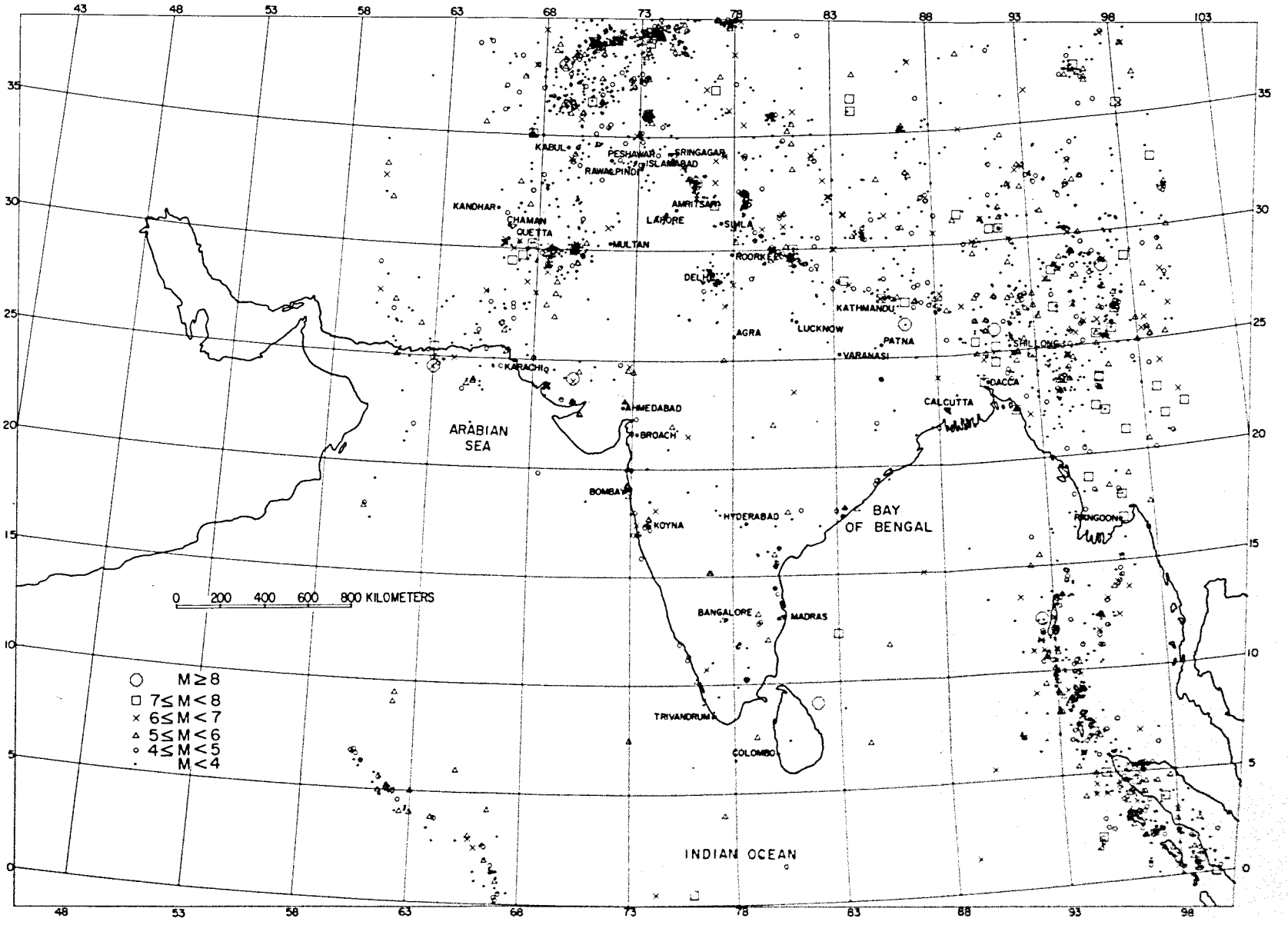

Fig. 1. Epicenters of shallow-focus earthquakes ($H \leq 70$ km). Sources of seismicity data are (1) NOAA's National Geophysical and Solar Terrestrial Data Center Catalog from 1900 through 1975, (2) the catalog compiled by Roorkee University (unpublished) for the period prior to 1900.

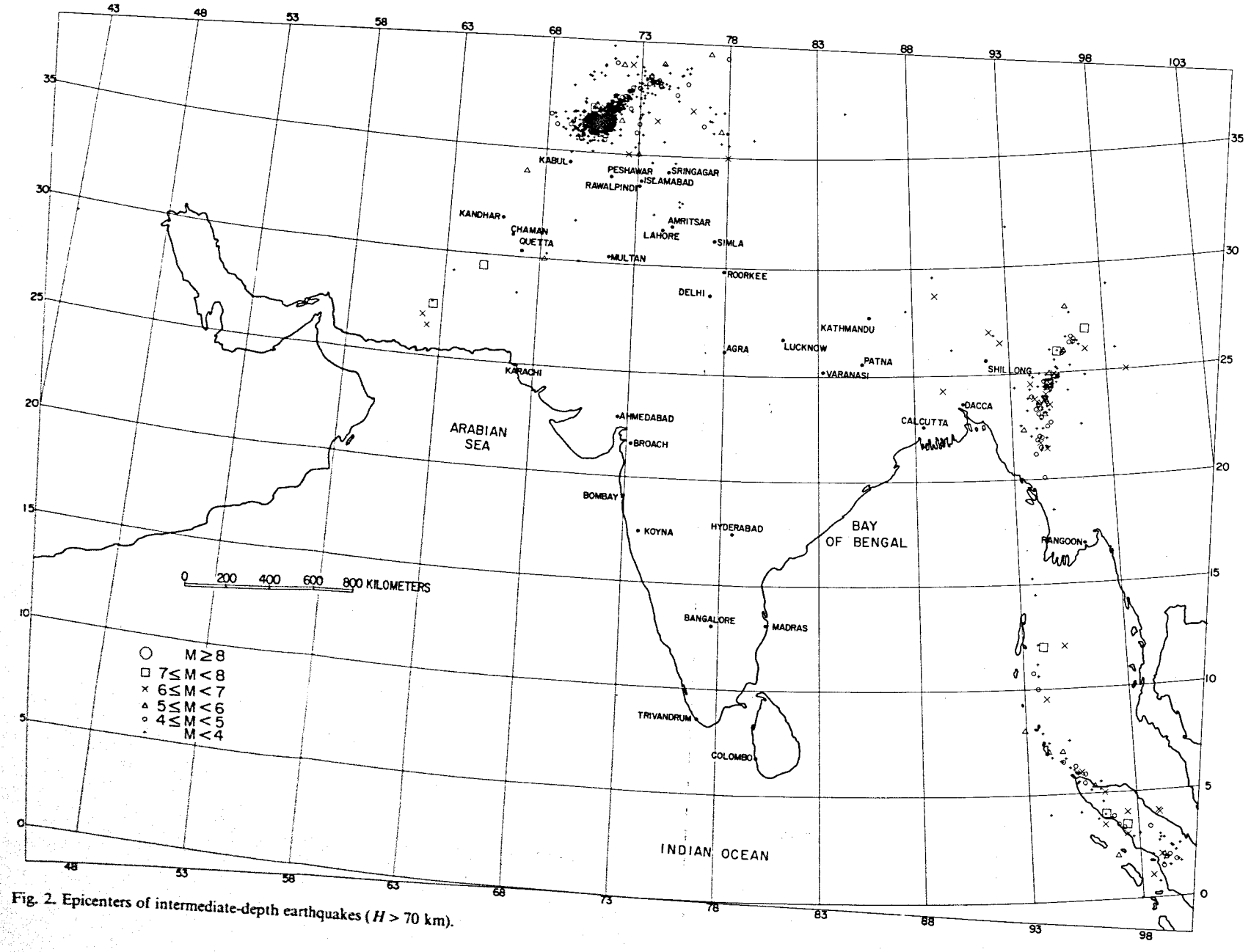

Fig. 2. Epicenters of intermediate-depth earthquakes ($H > 70$ km).

intermediate-depth earthquakes with depths greater than 70 km. Surface-wave magnitudes were used in the analysis. For recent earthquakes for which the NOAA or USGS report body-wave magnitudes, Richter's relation (Richter, 1958) was used to convert them to surface-wave magnitudes. The incompatibility of body-wave magnitudes in the Richter relation and those of NOAA-USGS would lead to some differences in the converted magnitudes for events after 1963 and for smaller earthquakes (Båth, 1977). This effect is not expected to seriously affect our hazard calculations.

The principal elements of a seismic hazard map are: (1) the statistical model employed; (2) the ground-motion parameter mapped and its attenuation with distance as a function of magnitude and depth of focus; (3) the definition of seismic source zones; (4) the recurrence intervals of earthquakes in each magnitude class; and (5) the maximum magnitude for each source zone. Each of these items, except the statistical model which has been described by Algermissen and Perkins (1976) and Algermissen et al. (1982), will be discussed below.

DISTANCE-ATTENUATION LAWS

Because of a lack of adequate instrumental observations of strong ground motion in India, a suitable attenuation law for the region is not available. Fortunately, a number of investigations have mapped intensity of shaking for major and medium-sized earthquakes (Oldham, 1883, 1899, 1926; Middlemiss, 1910; Stuart, 1920; Gee, 1934; Auden and Ghosh, 1934; West, 1937; Ramchandra, 1953; Gupta et al., 1969, 1972; Singh et al., 1976; Gosavi et al., 1977). Intensity, which describes the effects of ground motion on humans, construction, and the earth's surface, has often been used as a parameter to estimate seismic hazard. Where mitigation of hazard by structural design is desired, however, a better parameter for hazard estimation is peak acceleration or peak velocity. For this reason a number of attempts have been made to correlate intensity with acceleration (Gutenberg and Richter, 1956); however, at present, there is a difference of opinion among scientists regarding the use of intensities for estimating maximum ground acceleration (Neumann, 1954; Housner, 1965). Often the peak acceleration does not correlate well with the observed intensity, particularly in the far field.

In the present analysis, we adopted an approach in which the MMI (Modified Mercalli intensity)-versus-distance relations for the India region were compared with those for the eastern and western parts of the United States to determine if similarities exist. We assumed that if the intensity for Indian earthquakes attenuates in a similar fashion to either of the United States regions, then it is reasonable to assume that the acceleration–attenuation relation for that area of the United States could be applied in the Indian study.

Early studies utilized the Oldham and Rossi-Forel intensity scales. The reports of these studies covered the great earthquakes and contained a copious description of

damage and also a comparison of the Oldham scale with the Rossi-Forrel scale. This detailed information has enabled the present authors to approximately transform early intensity maps into the MMI scale. The intensity maps for earthquakes since the great 1950 Assam earthquake were prepared using the MMI scale.

Figure 3 shows the intensity (MMI) versus geometric mean distance for 7 Indian earthquakes ranging in magnitude from 7.1 to 8.7. The distance for each intensity level was determined by computing the equivalent radius of a circle equal in area to that contained within the isoseismal. The intensity attenuation curves for the eastern United States (EUS), Cordillera, and San Andreas areas of the U.S. are also plotted (Howell and Schultz, 1975). From these data it is clear that, on average, MMI for Indian earthquakes attenuates like that in the EUS. Because the EUS intensity attenuation fits the Indian earthquakes well, we have selected the acceleration–distance curves developed for the EUS in rock by Algermissen and Perkins (1976), for the seismic hazard analysis in the Indian region (Fig. 4). These curves are employed without accounting for variability in the attenuation–distance relation. The effect of including such variability in estimating seismic hazard would be to raise the mapped peak acceleration levels in the range of 4–40% g by about 25–40% and larger mapped accelerations by greater percentages (Algermissen et al., 1982).

The focal depth of the earthquake is a major variable affecting surface ground-motion distribution. The depth of focus affects the epicentral intensity as well as the near-field rate of attenuation with increasing epicentral distance. A number of workers have investigated this problem and proposed relationships between intensity, epicentral distance, and focal depth (Gutenberg and Richter, 1956; Medvedev, 1959). Unfortunately, little information on intensity for intermediate-depth earthquakes for the Indian region is available, although a number of the intermediate-de-

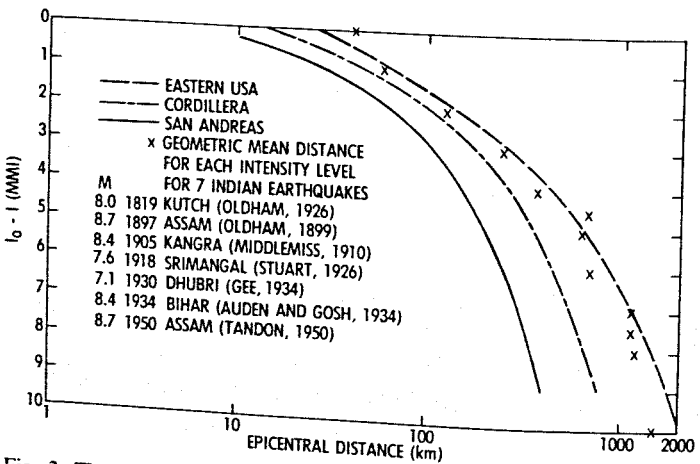

Fig. 3. The observed decay of intensity (MMI) with geometric epicentral distance for seven Indian earthquakes is shown with the intensity–distance attenuation relations for eastern, San Andreas and Cordillera areas of the U.S.A. (Howell and Schultz, 1975).

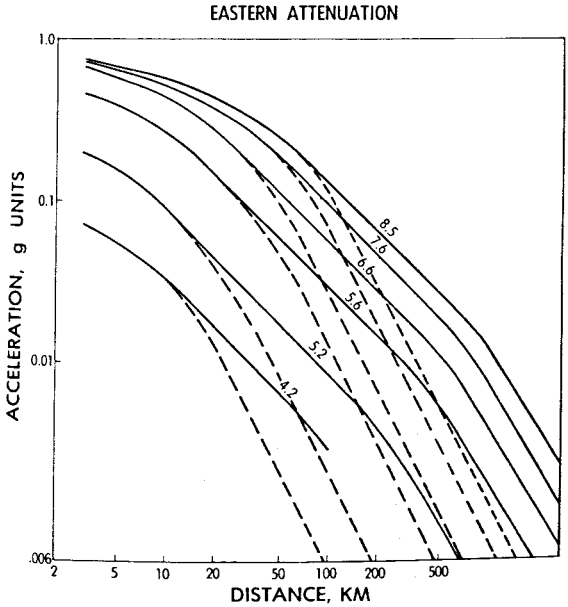

Fig. 4. The attenuation of peak acceleration in rock with epicentral distance is shown for shallow-focus earthquakes for the Eastern United States (solid line) and Western United States (dashed line) (Schnabel and Seed, 1973; Algermissen and Perkins, 1976). The eastern United States curve is employed in this study.

pth earthquakes, which occur in the northwestern and eastern parts of the region have produced damage (Gutenberg and Richter, 1965).

In the absence of empirical data and a firm theoretical analysis, a heuristic rationale was developed to derive acceleration–distance attenuation curves for intermediate-depth earthquakes from the curves for surface-focus earthquakes of Fig. 4. The intermediate-depth earthquakes would contribute little to the accelera- tion return periods if the energy focus of the earthquakes was assigned to the known hypocentral depths. Because it is known that some of these earthquakes cause damage, we assume that these energy foci on average have a shallower depth of focus than the hypocenter, i.e., that the earthquakes rupture toward the surface in a manner analogous to the behavior of shallow-focus earthquakes (McCann et al., 1979). Accordingly, all intermediate-depth earthquakes (depth 70–200 km) were assigned an effective depth of 100 km (fault length). In the absence of a magnitude- versus-fault relationship appropriate for intermediate-depth earthquakes, the fault lengths were estimated using a relationship for shallow focus earthquakes given by Bonilla and Buchanan (1970). Using the effective depth, source–site hypocentral distances were calculated corresponding to various epicentral distances. The values of acceleration were read off the graphs of Fig. 4 corresponding to the calculated

energy center distances and replotted at the corresponding epicentral distances to produce the desired acceleration–epicentral distance attenuation curves shown in Fig. 5. These curves show the expected behavior, viz., a slow decay of ground motion near the epicenter and a decay rate comparable to that for shallow-focus events at larger distances. The seismic hazard analysis for intermediate-depth events has been computed using the above curves. Similar assumptions in modeling the acceleration attenuation law for deep events were made by Båth (1975) for earthquakes in Tanzania. The shallow focus events ($H \leq 70$ km) were assumed to rupture to the surface in estimating the seismic hazard.

TECTONIC FRAMEWORK

At present a relationship between seismicity and the geological features can be established only in generalized form over fairly large areas. One reasonable working hypothesis that has been applied in the USSR employs data on recent vertical and horizontal tectonic movements to identify the areas of seismic potential (Bune et al., 1976). Where such data are not available, attempts are made to correlate seismicity with factors such as evolutionary history, faults of regional importance, distribution

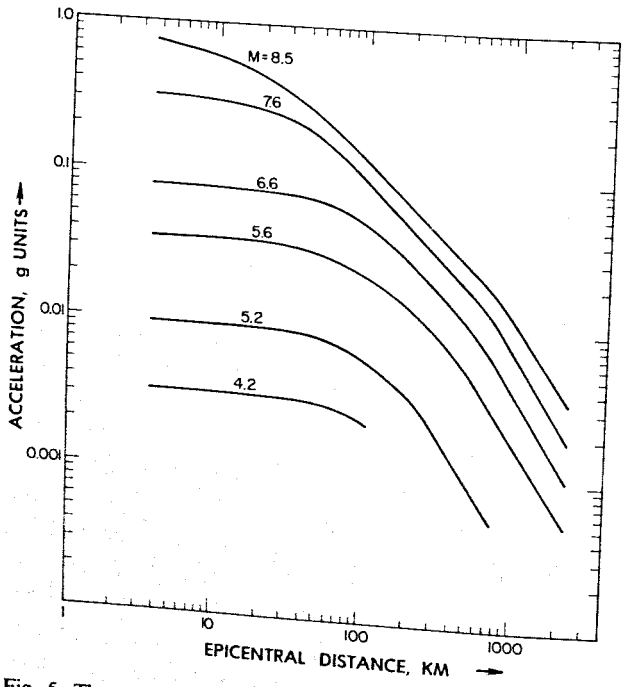

Fig. 5. The attenuation of peak acceleration in rock with epicentral distance for intermediate-depth earthquakes derived for this study.

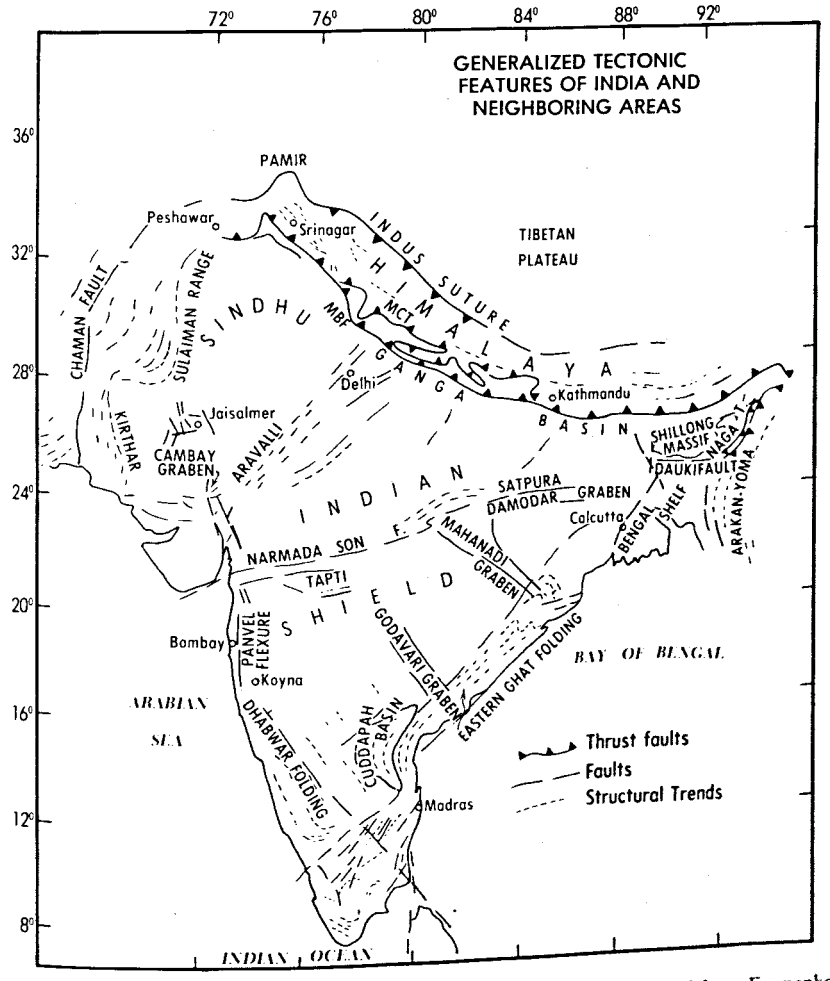

Fig. 6. Generalized tectonic features of India and neighboring areas (adapted from Eremenko and Negi (1968), Valdiya (1973) and Geological map of Asia and the Far East (UNESCO, 1971)).

of most recent movements, young volcanoes, etc. We have followed these general principles to demarcate seismic zones in this study. The historical seismicity of the region is shown in Figs. 1 and 2. A generalized tectonic map summarizing the main features of the region is shown in Fig. 6, and the source zones chosen on the basis of these data are shown in Fig. 7.

The Indian region may be classified into three main subdivisions on the basis of general geological and physiographical features. The mountain ranges constitute the first subdivision and consist of the Sulaiman and Kirthar ranges on the northwest. the Himalaya mountains on the north extending from east to west for a distance of

2500 km, and the Arakan-Yoma mountains ranging from north to south into the island arc system consisting of the Andaman Nicobar, Sumatra, and Java Islands. The average elevations in this subdivision range between 1000 and 4500 m. The second subdivision consists of the vast alluvial plains of the rivers Sindhu (Indus) and Ganga (Ganges) with an average elevation of about 200 m. The hills and coastal plains of the Indian peninsular shield comprise the third subdivision with an average elevation of about 600 m, although ranges are present within this region having elevations in excess of 2500 m.

The first subdivision represents a tectogene formed by the collision of the Indian and the Eurasian plates (LeFort, 1975). The middle to late Tertiary rock structures in this subdivision are highly folded and thrusted, have numerous nappes (Wadia, 1957; Gansser, 1964; Krishnan, 1968; Valdiya, 1973), and a high level of seismicity. The fault plane solutions indicate a general northward underthrusting of the Indian plate on the Himalaya front and an eastward underthrusting in the Arakan Yoma region in the east. The tectonics of the Kirthar–Sulaiman ranges is influenced by transcurrent faulting. Eleven seismic source zones (Nos. 7–10, 12, 14, 16, 18, 19, 24) have been identified within this subdivision on the basis of seismotectonics.

The Sindhu–Ganga (second) subdivision consists of the autochthonous zone in which the Precambrian rocks of the Indian shield are downwarped and plunge under the mountains towards the northwest, north, and east forming the foredeep and marginal depression south of the Himalaya tectonic zone. Major subsurface basement faults have been mapped in the area bordering the Himalaya mountains, which reflect the continuation of the tectonic features mapped in the peninsular shield (Eremenko and Negi, 1968; Valdiya, 1973; Sengupta and Khattri, 1975). Infrequent earthquakes occur in this subdivision and are clustered in a few localities. This subdivision, could possibly sustain tensional earthquakes, such as observed in ocean trenches (e.g., Stauder, 1968), anywhere along its length due to flexure of the Indian plate under the Eurasian plate (Molnar et al., 1973). On the basis of this geodynamic model, it might be preferable to define a single source zone paralleling the Himalaya mountains and encompassing the clusters of earthquakes observed historically. In the present study, however, an alternative model was adopted wherein emphasis was placed on historical seismicity, and, accordingly, source zones 15, 20, 21, and 22 were demarcated. As a consequence of this choice, the estimates of seismic hazard in these source zones will be higher compared to areas that are herein treated as zones of background seismicity.

Source zone 10 in the northeastern region occupies a special position in the tectonic framework of India. This zone encompasses the narrow Bramphaputra valley and the Shillong massif and has a record of very high seismicity. This zone is being underthrust to the north at the Himalayan front and to the southeast in the Arakan Yoma region and is under high compressive stress.

Source zones 1–5 and 11 are located in the Indian peninsular shield and coastal areas that constitute the third subdivision. Except for source zone 3 lying on the

western coast, the seismic activity in these source zones is weak compared to seismicity in the first subdivision. Although some of the fault plane solutions of earthquakes in this subdivision suggest north–south directed compressive stresses (Chandra, 1977) which may be generated by the plate collision in the Himalaya region, the seismotectonics locally may be governed by regional geologic structures defining particular zones. In the peninsula, a number of isolated earthquakes have been reported that lie outside the source zones drawn there. Detailed seismological and geological studies of the areas of isolated earthquakes are needed for investigating the possibility of incorporating additional source zones into the analysis.

The trans-Himalaya area in Tibet has been identified as a single large source zone (number 23) in the present study. Sri Lanka has not been included in any seismic source zone because there is a lack of reported seismicity, although one great earthquake ($M > 8$, 12/31, 1881, unpublished earthquake catalogue of the University of Roorkee) occurred in an offshore area of Sri Lanka. Aseismicity in this area appears to be real because the WWSSN station at Kodai Kanal (KOD) would have reported earthquakes if they had occurred.

SOURCE ZONES AND CHARACTERISTIC SEISMICITY

Source zone 1. This zone is comprised mainly of the eastern coastal belt and includes parts of the Mahanadi and Godavari grabens. The major part of the zone consists of Archean rocks and Precambrian fault systems. The general tectonic trend in this zone is in an east-northeast direction. It swings in a southerly direction to parallel the curvature of the eastern margin of the Cuddapah basin (79°E, 15°N) and again turns to assume a north-easterly alignment in the area south of Madras (80.3°E, 13.1°N.) (Eremenko and Negi, 1968; Valdiya, 1973). The coastal margins bear evidence of Mesozoic and Tertiary block faulting along southeast strikes. The zone is characterized by diffuse low magnitude shallow focus seismicity. Significant association of historical seismicity with mapped geological faults is not apparent. The area has experienced an occasional earthquake of magnitude 5–6, with the largest reported magnitude of 6. Fault plane solutions have been obtained for three earthquakes which occurred, respectively, near Midnapur (88.0°E, 21.7°N), Bhadrachalam (80.6°E, 17.9°N) and Ongole (80.1°E, 15.6°N). Using preferred solutions, all these events display one nodal plane with northeast–southwest orientation, paralleling the lineaments in the area, along which there was left-lateral strike-slip motion. The orthogonal nodal plane is aligned in a northwesterly direction. An alternative set of solutions showed thrust faulting along northwest trending fault planes (Chandra, 1977).

Source zone 2. The western coast of India extending from Koyna on the south to Ahmedabad on the north has occasionally had moderate earthquakes. The geology of the region features extensive lava flows (known as Deccan Traps) of late Mesozoic–early Tertiary age which, at places, attain great thickness (1000 m or

more) (Raju, 1968; Avasthi et al., 1971). On the north, a north-northwest-trending (Cambay) graben is filled with thick Tertiary sediments and Tertiary and Quaternary synsedimentary faulting. A major tectonic feature of lower Miocene age called the Panvel flexure runs in a northerly direction extending from latitudes 16°N to 21°N. A series of hot springs are located along this flexure which parallels the ancient Aravalli trend inferred to underlie the area (Krishnan, 1968). Burke and Dewey (1973) suggest that the tectonic framework of the area has been influenced by a hot spot or a mantle plume in the Mesozoic. The associated doming and uplift of the crust has continued at least up to the Quaternary (Gubin, 1968). These tectonic features are related to the rifting and subsequent transport of the Indian landmass from Gondwanaland. Another major lineament, the nearly east-trending Narmada rift (Auden, 1969), intersects this source zone on the north. Near Broach, Tertiary age normal faulting along this lineament is recognized (Mathur et al., 1968). The most recent significant earthquakes in zone 2 have been the Koyna dam earthquake of December 1967 ($M = 6.2$) and the Broach earthquake of 1970 ($M = 5.4$). Other notable earthquakes are the Bombay earthquake of 1618 of intensity IX (?), the Bombay–Surat earthquake of 1856 of intensity VII, the Mahabaleshwar earthquake (73.3°E, 17.9°N) of 1764 of intensity VII, and the Ahmedabad earthquake (72.8°E, 22.3°N) of 1864 ($I_0 = \text{VII}$) (Chandra, 1977). The Broach earthquake (73.0°E, 21.7°N) was located on the intersection of the Narmada rift and Cambay graben. One of the nodal planes was parallel to the Narmada rift trending in an east–west direction (Gupta et al., 1972). The 1967 Koyna earthquake (73.7°E, 17.5°N), which may have been induced by filling a reservoir, displayed a north-northeast and northwest-trending pair of nodal planes with dominant left-lateral strike-slip motion (Chandra, 1977). The north-northeast-trending plane is the preferred fault plane. The seismicity in this zone is confined to shallow crustal depths.

Source zone 3. The Kutch region is a major zone of shallow-focus seismic activity, second in activity only to the active plate boundary zones. The major tectonic features align in a west-northwest direction and within these features block faulting has formed a system of nearly east-trending grabens and ridges. This tectonic lineament is almost orthogonal to those existing in adjacent source zones and was formed in the late Mesozoic or Tertiary.

A severe earthquake ($I_0 = \text{XI}$) that occurred in 1819 was accompanied by the formation of a ridge near Lakhpat (68.7°E, 23.7°N) trending in an easterly direction. The ridge was 24 km wide and 10 km long with elevation changes of several meters (Oldham, 1883). Another significant earthquake occurred at Anjar (70.0°E, 23.0°N) in 1956, with $M = 6.1$ and $I_0 = \text{IX}$.

Source zone 4. This zone is associated with the northeast-trending Arravali range, consisting of rocks of the Archean Arravali and Delhi systems. The seismicity in this zone consists of low magnitude shallow-focus events. An earthquake with epicentral intensity of VII was reported in Mount Abu in 1848. An earthquake having $m_b = 5$ occurred near Mt. Abu (72.4°E, 24.8°N) in 1969. The fault-plane solution for this

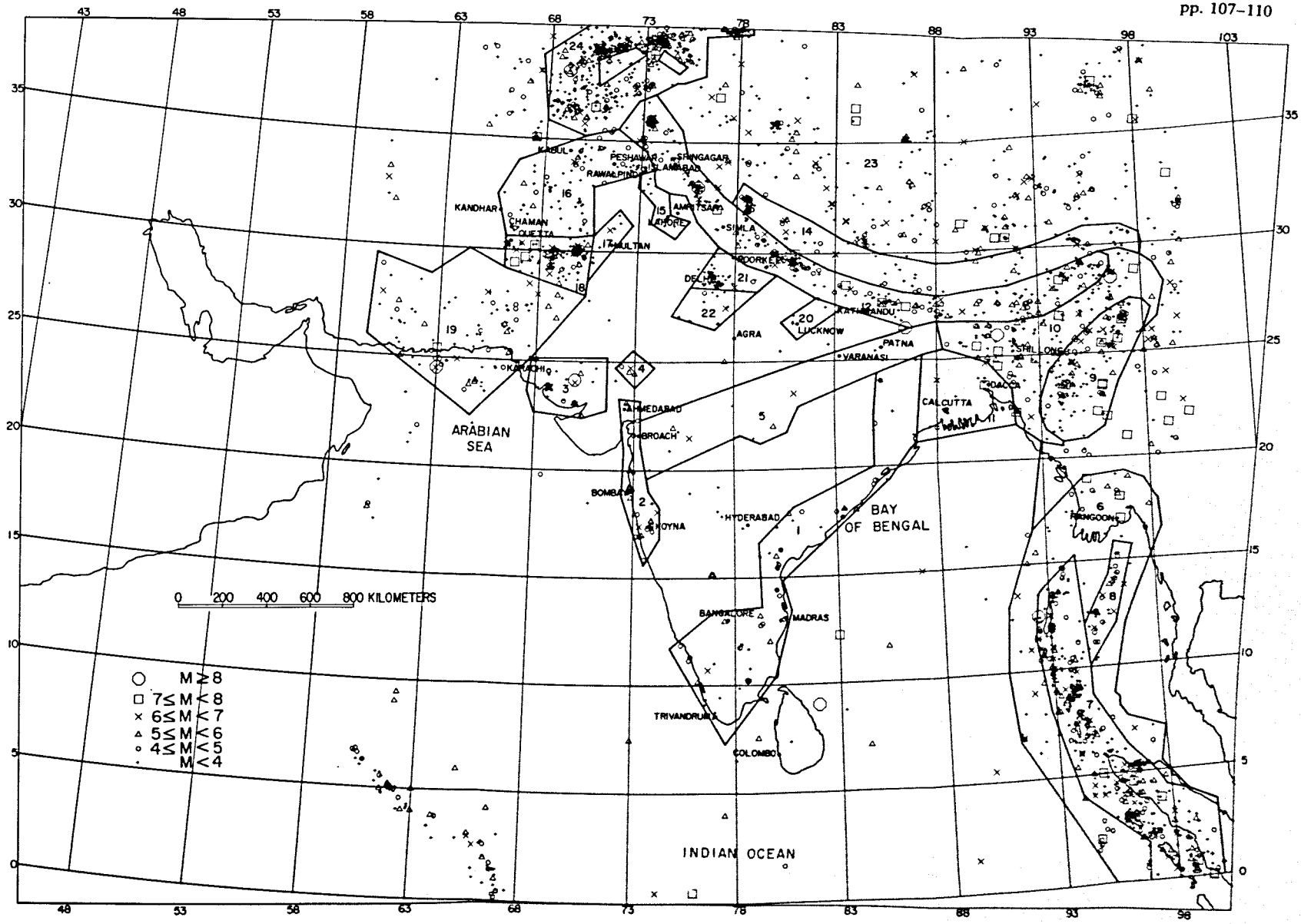

Fig. 7. Source zones that were used to prepare the seismic hazard map.

shock displayed a northwest- and east-northeast-trending pair of nodal planes. The latter trend, which is nearly parallel to the Arravali fault system exhibits a thrust solution with a component of left-lateral strike-slip motion (Chandra, 1977).

Source zone 5. This zone encloses the Narmada–Tapti rift, a system of deep-seated faults of regional significance (Naqvi et al., 1974). Considerable vertical movements on these faults have created wedges of basement that are surrounded by younger geological formations. Although the rift is of Precambrian age (McConnell, 1974), there may be young faulting along some segments; for example, in the Broach area (western extremity) faulting may have continued into the Pleistocene (Auden, 1959). The more notable earthquakes are the Son Valley earthquake (81.0°E, 23.5°N) of 1927 ($M = 6.5$), the Satpura earthquake (75.7°E, 21.5°N) of 1938 ($M = 6.3$) and the Balaghat earthquake (80°E, 22°N) of 1957 ($M = 5.5$). The seismicity is confined to shallow crustal depths.

The great 1934 Bihar earthquake ($M = 8.4$) occurred near the junction of this zone and zone 12 in Himalaya. This earthquake had three zones of maximum intensity XII, one of which was in zone 12. We have associated this event with seismic zone 12, the principal seismic zone of the Himalaya tectonic province.

Source zones 6, 7, and 8. Geologically, the Andaman–Nicobar Islands were developed due to the convergence of the Indian and Burmese crustal plates, producing an anticlinal welt with faults parallel to the island structure. A simple plate model, however, does not account for all the facets of the modern seismicity (Sinvhal et al., 1978). The fault plane solutions indicate normal faulting such that the V-shaped area between source zones 7 and 8 forms a graben (Fitch, 1970, 1972; Ichikawa et al., 1972).

The seismicity of this island arc system has been divided into three zones. Zone 6 defines the outer margins of the seismic belt that consists of only shallow-focus events. The seismicity is also somewhat less intense in this zone compared to the central portion, which is designated zone 7, where both shallow and intermediate-depth earthquakes occur. A distinct band of seismicity trending in a north-northeast direction on the inner side of the island arc system has been delineated as zone 8. Here, too, only shallow-focus earthquakes are reported.

There have been several major earthquakes in this area, the most significant being the great earthquake of 1941 ($M = 8.7$) in zone 7. Seven shallow earthquakes and five deep earthquakes with magnitudes in the 7–8 range have been reported in this zone. By comparison, in zone 6 in the present century, only three major shallow earthquakes ($7 \leq M < 8$) have occurred, of which the largest was $M = 7.7$. The largest earthquake in zone 8 had a magnitude of 6.7.

Source zone 9. The highly seismic region of the Arakan Yoma fold belt consists of large thicknesses of Mesozoic and Tertiary rocks intruded by granitic and ultra basic rocks (Krishnan, 1968). The arcuate northerly-trending geological province is a highly folded allocthonous zone. It is the northward continuation into the continent of the Andaman, Nicobar, Sumatra, and Java island arc system (Sunda arc) and is

laced with thrust zones and other faults that have been produced by the collision of the Indian and Burmese plates (Deshikacher, 1974; Verma et al., 1976). In this area there is a Benioff zone dipping towards the east with earthquake hypocenters ranging in depth down to about 250 km. The fault-plane solutions indicate east–west-directed thrusting and confirm the concept of a plate collision boundary (Chandra, 1977). Some fault-plane solutions also indicate strike-slip motion (e.g., Verma et al., 1976). The largest recorded earthquakes in this zone have had magnitudes less than 8. Although four shallow and six intermediate events with $7 \leq M < 8$ have been reported in the past, the largest reported magnitude is 7.75 for shallow earthquakes and 7.0 for intermediate depth earthquakes.

Source zone 10. The Brahmaputra valley constitutes one of the most seismically active areas on the subcontinent. It is bordered on the north by the frontal Himalayan ranges and to the southeast by the Schuppen belt of the Naga Hills and the Arakan-Yoma ranges. To the east the lower Bramhaputra valley is characterized by recent alluvial cover that conceals considerable thickness of Tertiary sediments. The Shillong massif is an important geologic unit in this area and is believed to have been uplifted in the Miocene (Krishnan, 1953). The structure of this massif is characterized by systems of east-, northwest, and north-trending basement faults and fractures. Although the area is traversed by faults with diverse strikes, the most prominent among them are the Dauki fault demarcating the southern edge of the massif, the Haflong fracture zone, and the Naga thrust directed towards the northwest on the southeastern edge of the Bramhaputra valley (Geological Survey of India, 1974). A difference of opinion exists as to the nature of slip on the Dauki fault. According to Evans (1964), it is a strike-slip fault with dextral motion, whereas Murthy et al. (1969) believe it to be a vertical fault without a horizontal component. Chandra (1978) has obtained fault-plane solutions of two earthquakes on this fault system and has interpreted a northward underthrusting along a east-trending fault plane. The great Assam earthquake of 1950 had been interpreted to have a considerable strike-slip component along a west-northwest-trending fault plane (Ben Menahem et al., 1974). Another tectonic feature is the northwest-trending Mishmi thrust on the northeastern edge of the region near the Himalayan syntaxis. There was reactivation on these faults during the Pliocene as a result of the intense East Himalayan Orogeny (Geological Survey of India, 1974).

The tectonic regime can be summarized as a south-directed overthrusting from the north and a northwest-directed overthrusting from the southeast. These two oppositely directed force systems are likely to produce high levels of tectonic stress in this zone, and seismicity is well distributed throughout the region.

This zone has had two great earthquakes with magnitudes of 8.7 (1897 and 1950) in the past 80 years. The 1897 earthquake, which had its epicenter in the Shillong massif, produced accelerations in excess of 1 g (Oldham, 1899). In addition, there have been six other major earthquakes with magnitudes in excess of 7, some of which caused widespread destruction. The earthquakes are generally confined to the upper 80 km.

Source zone 11. This zone consists of an alluvium-covered geosynclinal basin. Due to a thick section of sedimentary cover, no structures are apparent on the surface. Geophysical surveys have revealed a system of normal faults in the sediments trending in a north-northeast direction with a hinge zone passing close to Calcutta (Sengupta, 1966). The current seismicity is relatively low, although the area seems to have been more active in previous centuries. The highest reported epicentral intensities are X in 1737, IX in 1842, VII in 1866 (Oldham, 1883). A damaging earthquake with $M = 5.7$ occurred in the area in 1969.

Source zones 12 and 14. The Himalaya tectonic unit, comprising the world's highest mountain chains, is contained in source zones 12 and 14. Although much of this area has a low population density, the importance of considering these zones stems from the large hydroelectric and other developmental projects undertaken there and in adjacent territories in recent times.

Structure within the Himalaya orogenic zone is dominated by numerous east-trending thrusts (Gansser, 1964; Valdiya, 1973; LeFort, 1975; Geological Survey of India, 1979). Three of these thrusts, namely the Counter Thrust or Indus Suture zone, the Main Central Thrust, and the Main Boundary Fault (MBF), extend continuously from east to west. Transverse faults cutting across the Himalaya tectonic province have also been recognized. These generally align parallel to and in continuation with the ancient tectonic lineaments present in the peninsular shield on the south (Valdiya, 1973). Thrust faulting, indicated by fault plane solutions, occurs along planes dipping gently towards the north and northeast in consonance with the convergent movement at this plate boundary (e.g., Chandra, 1978). Fault plane solutions generally indicate a northeast-directed compressional axis that conforms to the plate model.

The seismic activity in this province occurs in two narrow zones which follow the arcuate mountain belt. The main locale of seismicity (zone 12) follows the Central Himalaya ranges close to the Main Central thrust. It is interpreted to be associated with the Main Boundary thrust and related thrust faults. Zone 14, a zone of weaker seismic activity, occurs to the north of zone 12 and is likely caused by the same underlying thrust forces. The main criteria defining these zones is the intensity of historical seismicity. The main seismic zone, which we have designated source zone 12, continues along the entire length of the Himalaya tectonic province. Zone 14 has been drawn to encompass the secondary seismic belt to the north. The seismic activity in this zone decreases towards the west.

In zone 12, several major earthquakes, including the 1905 great Kangra earthquake ($M = 8.6$), have occurred. The meizoseismal area was associated with the MBF. The great 1934 Bihar earthquake ($M = 8.4$), about 1300 km to the east, occurred at the southern boundary of this zone near zone 5. The occurrence of a large earthquake near the junction of tectonic lineaments suggests an increase in seismic hazard in these locales (Gorshkov, 1974).

Six other very large earthquakes ($7 \leq M < 8$) are also reported in the historical data. The largest earthquakes seem to be associated with the southern margin of the source zone, which is characterized by the MBF discussed above.

Seismic source zone 14 is, by comparison, only moderately active, with magnitudes of historical earthquakes being less than 6.75. On the northwest and southeast extremes of these zones, significant intermediate-focus seismic activity also occurs.

Source zone 15. This zone is defined by a narrow linear belt of low magnitude earthquake foci parallel to and south of zone 12 in the westernmost sector. The area is covered with alluvium, which conceals thick Miocene sediments overlying the basement complex. The maximum magnitude reported here is 4.3. This seismicity may be produced by thrust faulting parallel to the thrusts in the Himalaya.

Source zones 16, 18 and 19. These three source zones occupy the Kirthar–Sulaiman mountain ranges in the northwest part of the Indian subcontinent. Epicentral zones follow the folded belt characterizing the area. The ranges consist of numerous Mesozoic and Tertiary arcuate faults and imbricated structures (Krishnan, 1968). A major fault system known as the Chaman fault, that is active along its entire length, runs in a general north-northeast direction. This region has been subdivided into three source zones on the basis of the intensity of historical seismicity. Of the three source zones, zones 18, which spans the arcuate ranges, and 19 are the most active. The maximum magnitude events in source zones 16, 18, and 19 are 6.4, 7.5, and 8.3, respectively. Only shallow-focus seismicity occurs in zones 16 and 18, while zone 19 contains both shallow- and intermediate-focus earthquakes. The geodynamic processes in these source zones are much more complicated than those of the Himalaya province. In contrast to the tectonic style in the Himalaya, where the dominant mode of tectonics is thrusting, transcurrent motion on the Chaman fault has a major influence on the tectonics of this region.

Source zone 17. This zone corresponds to a localized group of earthquakes that extends in a northeast direction from zone 18. The zone is an alluvial-covered tract characterized by shallow infrequent earthquakes. The maximum reported magnitude reported here is $M = 6.4$.

Source zones 20, 21 and 22. These three source zones are at the northern edge of the Indian shield and are adjacent to the Himalaya tectonic province. These areas are for the most part blanketed by alluvium and sediments of the Sindhu Ganga basin; however, the geology is exposed towards the southwest. Zones 21 and 22 coincide with the northeast end of the north-northeast-trending Aravalli rocks. The northeasterly continuity of these Archean rocks is intersected by the Himalaya mountains. These rocks form the basement and are characterized by complex faults and folds of Precambrian age. The zones have had relatively low seismicity in the past, with the largest reported event having a magnitude of about 6. Similarly, zone 20 is also characterized by low-magnitude seismicity and is associated with northeast-trending faults in the basement that have been delineated by geophysical mapping techniques (Sengupta and Khattri, 1973). These areas are of singular

importance because they are at the intersection of major tectonic lineaments. Such knots are believed to be zones particularly susceptible to major earthquakes in areas of active tectoncis (Gorshkov, 1974). These zones, therefore, are believed to have considerable seismic potential.

Source zone 23. The trans-Himalayan zone, extending up to latitude 38° on the north and longitude 100° on the east, has been treated as a single source zone. It is recognized that this vast region consists of varying geotectonic provinces and associated seismicity. However, in view of the remoteness of this source zone from population centers and from the area of primary concern in this work, greater subdivision would require a detailed investigation and was considered beyond the scope of the present study. The area is quite active seismically and has experienced as many as eighteen earthquakes with $7 \leq M < 8$ in the past hundred years; the largest event had a magnitude of 7.9.

Source zone 24. The Pamir knot, well known for intense shallow and intermediated-depth, seismic activity, constitutes source zone 24. The area is characterized by the junction of several tectonic provinces having very complicated geodynamic relationships: the Himalaya, the Tien-Shan, and the Kara Korum. The area has been shaken by four great earthquakes of magnitude in excess of 8, the largest being 8.6.

SELECTION OF THE PROJECTED MAXIMUM MAGNITUDE OF AN EARTHQUAKE IN EACH SOURCE ZONE

The choice of the maximum magnitude of an earthquake that can occur in a source zone can have an important effect on the peak accelerations expected in certain cases. For example, although at a given return period peak acceleration (a_p) is strongly dependent on the choice of maximum magnitude (M_{max}) for intermediate values of M_{max} (6), a_p is largely insensitive to M_{max} for large M_{max} (8 +) (Perkins, 1978). In this study many source zones have high M_{max}, and, consequently, variations in M_{max}, in these cases, are not expected to significantly affect a_p at a given return period. The rationale followed in assigning the maximum magnitude of an earthquake depends on several factors, including the maximum magnitude earthquake experienced in the past, the tectonic history, and the geodynamic potential for generating earthquakes. The projected maximum magnitudes of earthquakes for all the source zones are listed in Table 2 (p. 126). The maximum magnitude for intermediate-depth earthquakes has been assumed to be equal to the largest historical earthquake in the respective zone. A discussion of the maximum magnitude for shallow earthquakes follows.

In source zone 1, the maximum reported magnitude is 6, while the maximum projection of 7 is based on the existence of basin-producing Tertiary tectonics. In the case of source zone 2, historical data show that the maximum intensity experienced here was only IX(?). The geological data, however, indicate that there has been recent tectonic activity. In view of the tectonic framework, a maximum expected

TABLE 1

Earthquake parameters for source zones

Zone No.	Shallow-focus earthquakes ($H \leq 70$ km)				Intermediate-depth earthquakes ($H \geq 70$ km)				Remarks
	a	b	M_{max} observed	M_{max} projected	a	b	M_{max} observed	M_{max} projected	
1	4.22 $M \leq 6$	−0.787	6.0	7.0	–	–	–	–	(1) from combined analysis of 1–5, 11, 15, 17, 20, 21, 22
	4.22 $6 < M \leq 7$	−0.787	–	–	–	–	–		
2	4.18 $M \leq 6$	−0.787	6.8	8.0	–	–	–		(1)
	4.18 $6 < M \leq 7$	−0.787	–	–	–	–	–		
	4.27 $M > 7$	−0.787	–	–	–	–	–		
3	5.09 $M \leq 6$	−0.787	8.0	8.0	–	–	–		(1)
	5.09 $6 < M \leq 7$	−0.787	–	–	–	–	–		
	5.18 $M > 7$	−0.787	–	–	–	–	–		
4	4.22	−0.787	6.0	6.0	–	–	–		(1)
5	4.13 $M \leq 6$	−0.787	6.5	8.0	–	–	–	–	(1)

	4.13 $6 < M \leq 7$								
	4.22 $M > 7$								
6	4.31	−0.533	7.7	8.5	–	–	–	–	max slope and a value from 6 alone
7	5.44	−0.678	8.7	8.75	3.99	−0.521	7.2	7.5	from 7 alone for shallow
8	4.37	−0.580	6.7	7.0	–	–	–	–	from 6 + 8 + 9
9	4.52 $M \leq 7$	−0.580	7.8	8.0	4.64	−0.571	7.0	7.0	from 6 + 8 + 9
	$M > 7$	4.65							
10	3.78	−0.447	8.7	8.75	2.76	−0.437	7.0	7.0	from 10 alone
11	4.42 $M \leq 6$	−0.787	7.3	8.0	–	–	–	–	(1)
	$6 < M \leq 7$	4.43							
	$M > 7$	4.52							

TABLE 1 (continued)

Zone No.	Shallow-focus earthquakes ($H \leq 70$ km)				Intermediate-depth earthquakes ($H \geq 70$ km)				Remarks
	a	b	M_{max} observed	M_{max} projected	a	b	M_{max} observed	M_{max} projected	
12	5.65	−0.757	8.6	8.75	2.62	−0.437	6.75	7.0	from 12 alone
14	4.37	−0.613	6.75	8.0	2.32	−0.437	> 6.0	7.0	from 14 alone
15	3.44 $M \leq 6$	−0.787		7.0	–	–	–	–	(1)
	3.44 $6 < M \leq 7$								
16	3.73	−0.581	6.4	8.0	–	–	–	–	16 + 18 + 19
17	4.22 $M \leq 6$	−0.787	6.5	7.0	–	–	–	–	(1)
	4.22 $6 < M \leq 7$								
18	3.96	−0.485	7.5	8.0	–	–	–	–	from 18 alone
19	3.75 $M \leq 7.5$	−0.581	8.3	8.5	3.06	−0.437	7.0		16 + 18 + 19
	4.46 $7.5 < M \leq 8.0$								
	4.74 $M > 8.0$								
20	3.44 $M \leq 6$	−0.787	5.5	8.0	–	–	–	(1)	

	3.44 $6 < M \leq 7$								
	3.54 $M > 7$								
21	4.53 $M \leq 6$	−0.787	6.0	8.0	–	–	–	(1)	
	4.53 $6 < M \leq 7$								
	4.62 $M > 7$								
22	3.44 $M \leq 6$	−0.787	6.0	8.0	–	–	–	–	(1)
	3.44 $6 < M \leq 7$								
	3.54 $M > 7$								
23	4.83	−0.543	7.9	8.5	–	–	–	–	from 23 alone
24	4.59	−0.561	8.6	8.75	5.29	−0.602	8.1	8.1	from 24 alone

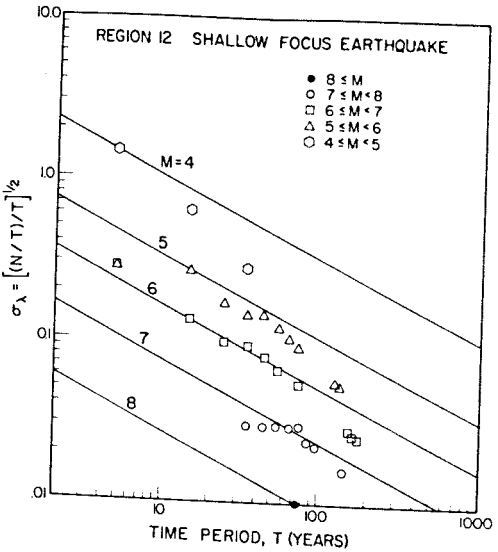

Fig. 8. Standard deviation of the estimate of the mean of the annual number of events (s_g) as a function of sample length (T) and magnitude (M).

magnitude of 8 has been chosen for this source region. The observed and projected magnitudes are the same as reported in historical times for source zones 3 and 4. The maximum magnitude projected for source zone 5 is 8 compared with the historically observed value of 6.5. This increase was chosen in recognition of the deep-seated nature of the Narmada rift and its repeated reactivation.

A marginal upgrading of the value of the projected maximum magnitude earthquake as compared to the maximum observed has been assumed for source zones 6, 7, 8, 9, 10, 12, 18, 19, and 24.

Maximum magnitude earthquakes, significantly higher than historically reported earthquakes have been selected for source zones 15, 17, 20, 21, and 22. These zones lie to the south of the main Himalaya seismogenic province. These zones represent locales where new fractures can take place by the bending downwards of the crust on account of the convergence of the Indian and the Eurasian plates in the manner of the tensional earthquakes that occur in subduction zones (Molnar et al., 1973). Furthermore, zones 21–22 lie near the intersection of tectonic trends. A value higher than the historical magnitude, therefore, seems to be appropriate in these cases. The maximum magnitude of the earthquakes in source zones 14, 16, and 23 has been assumed on the basis that these source zones lie in the midst of seismogenic provinces that are capable of supporting great earthquakes.

PARAMETERS FOR RECURRENCE RELATIONS

The catalog of earthquakes maintained by NOAA and supplemented by the earthquake catalog prepared by Roorkee University forms the basis of the analysis

of recurrence relations. Although the historical data go as far back as the late 16th century, the reporting is not homogeneous. The records for source zones 1, 2, 3, 9, 10, 11, 12 and 22 span a relatively long time period (from the 16th century), whereas for other zones the record is comparatively short, going back only as far as 50 years or so.

Earthquake catalogs are often biased due to incomplete reporting for both smaller earthquakes and also for large earthquakes having very long return periods. The estimates of recurrence parameters a and b can be in considerable error if due consideration is not given to these limitations of the data. In this study, an attempt is made to use the rates associated with that portion of the data set that is homogeneous by comparing observed seismic rates with the expected properties of a homogenous data set (Stepp, 1973). Figure 8 illustrates an example of this process for source region 12 for shallow earthquakes where a complete record would plot with a slope of $1/\sqrt{T}$ in each magnitude range and have a constant offset between magnitudes. Here it is seen that $M = 4$ may not be complete; $M = 5$ is complete for the last 50 years; $M = 6$ is complete for the last 70 years; $M = 7$ is complete for the entire period; and the completeness for $M = 8$ cannot be determined.

After correction for completeness, insofar as possible, the interval-recurrence relation was determined for each source zone; and from this relation, the cumulative recurrence curve was established (Herrmann, 1977). Although other methods have been suggested for deriving the cumulative recurrence curve (Båth, 1978, 1981), the method used here seems to be adequate for our data set. The results of this analysis are listed in Table 1.

One difficulty encountered in the present study is the low level of seismicity for some of the source regions. Most of these source regions occur in the relatively stable Peninsular shield; although the historical seismicity shows that these areas have definite potential for seismic hazard, the sparse data preclude an individual statistical analysis for each region. In the absence of a better solution, the historical seismicity data for source zones 1–5, 11, 15, 17 and 20–22 were merged for the purpose of estimating coefficients appearing in the recurrence relation. The rationale behind this procedure is that because all these source zones characterize intraplate earthquakes (with the possible exception of zones 15 and 17), it is assumed that they respond to similar stresses in the same fashion. In the same manner, a combined analysis was also performed for regions 6, 8, and 9, and for 16, 18 and 19 for shallow earthquakes and for 10, 12, 14 and 19 for intermediate-focus events.

After a recurrence relation was determined for the merged data, the seismicity represented by the relation was redistributed to each source region entering into the analysis. In this process, it is assumed that the b value remains the same in all the regions and only an appropriate a value is to be assigned. Although a number of alternative procedures for performing this redistributed were investigated, we chose the following one.

We use the estimated b-value to get an a-value for each magnitude interval in a

region. Thus, for each region there were as many a-values as there are magnitude intervals with observed earthquakes. Next, we converted each region's a values into total number of earthquakes ($M > 0$) and took the average to get an average a-value. The resulting a-values for the regions were then used to calculate the total number of earthquakes for a given M for each region. These numbers were used to set the proportions with which the seismicity for the merged zones was redistributed to the constituent zone.

By choosing a magnitude interval in which it is expected that reporting would be reasonably complete, the most reliable estimates of the reapportioned seismicity will be made. In the present analysis, therefore, we followed this procedure using three magnitude interval mid-points at 5.5, 6.5, and 7.5, to obtain an average estimate for a in each region.

The regions considered in the analysis have different maximum magnitudes. Therefore, this redistribution process produced different effective a values for different segments of the magnitude scale for some source zones (see Table 1), leading to discontinuous recurrence curves in these instances. This situation is an artificial one imposed by the necessity of combining various source zones for the estimation of recurrence parameters, but conserves the total number of earthquakes predicted by the fit of merged-zone data.

The magnitude–frequency laws derived by least-squares regression on the data are illustrated in Fig. 9 for three cases that represent examples of a good data set for shallow earthquakes, a poor data set of merged shallow events, and another good data set for intermediate-depth events. Analysis of the data in this fashion showed that, even after correction for incompleteness, bias due to incomplete reporting of earthquakes for $M \leq 6.0$ remained for several source regions [(1-5, 11, 15, 17, 20-22), (6, 8, 9), (16, 18, 19), 7 intermediate, 9 intermediate]. Incomplete magnitude classes were excluded from a and b value determinations.

Perkins (1978) has performed simulation studies to evaluate the sensitivity of the estimates of acceleration hazard to variations in seismicity parameters such as a- and b-values, the maximum expected magnitude, the grid size used, and the finiteness of sources. His analysis shows that seismic activity rates are relatively less critical in the analysis if the accelerations levels are high. For example, an increase in seismicity by a factor of 2 would cause an increase in accelerations at a given return period of 10% if the accelerations are high and 30% if they are low. Similarly, a variation of one standard deviation (about 0.1) in the b-value causes a 50% variation in accelerations at low levels and about 30% variation at high levels. Therefore, the results are more sensitive to the b-value. A somewhat redeeming feature of estimating a- and b-values jointly from empirical data is that an increase in the estimate of the a-value is accompanied by an increase in the estimate of the b-value and vice versa. Because an increase in the a-value decreases the return period of a given level of acceleration while an increase in the b-value increases it, the two results are to an extent self-compensating. We note that the a and b parameters for all zones in the present

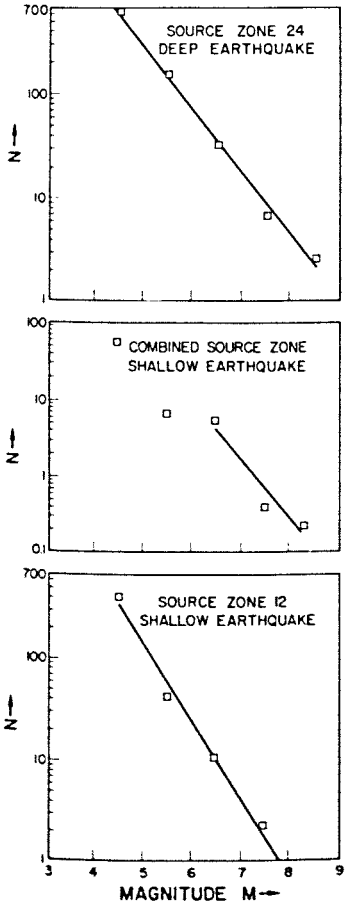

Fig. 9. Three examples of recurrence relations (log $N = a - bM$) showing the quality of the data.

study have been estimated from the observed data and are considered reliable in most cases (except source zones 7 deep, 6, and 8). The estimates of the peak accelerations, therefore, are expected to be relatively unaffected and insensitive to errors in a and b, especially in the most seismically active areas.

FINITE RUPTURE SOURCES

Representing large earthquakes by a series of point sources to model fault traces on the surface and using point attenuation functions leads to an underassessment of the frequency of occurrence of large accelerations and an overestimation of small accelerations near the fault (Algermissen and Perkins, 1976). This deficiency is corrected by representing sources as lines rather than points and utilizing attenuation curves that decay away from the fault trace rather than the epicenter. The

iso-peak acceleration contours in this case align parallel to the fault for a length appropriate to the magnitude.

The effect of rupture sources rather than point sources was included by specifying generic fault lines that were assumed parallel to the regional tectonic lineaments and were spaced approximately 20 km apart throughout a source zone. In addition, the known major faults were treated separately in each zone. At the ends of the fault rupture, semicircles were used to represent the acceleration contours. The seismicity was distributed among point sources and faults in the following manner. Seismicity up to magnitude $M < 6.5$ was distributed as point sources uniformly in a zone. The seismicity between $6.5 \leq M < 7.5$ was located on the generic faults, and events with $M \geq 7.5$ were assigned to the major important faults. These faults were identified from the Tectonic Map of India (Eremenko and Negi, 1968), the Geological Map of Asia and Far East (UNESCO, 1971) and Gansser (1964). Identification of major faults was based on age and length of faulting, on the occurrence of major historical earthquakes in proximity to the fault, and on the potential of a fault for a major earthquake based on knowledge of its tectonic setting. In the calculations, major faults were treated as fault zones by drawing two or more fault traces parallel to the mapped fault with a spacing of roughly 20 km. This model greatly increases the likelihood that a high acceleration will be experienced at a point, as compared to that likelihood obtained using point sources.

In source zone 12, located within the Himalaya tectonic province, numerous thrusts intertwine along the length of the zone. The greatest earthquakes, however, occur on the southern edge of this zone where the Sindhu–Ganga alluvial plains abut the Himalaya. This region marks a considerable physiographic elevation change that could also produce stress differentials. On this basis, we consider the Main Boundary Fault capable of sustaining high stresses and producing great earthquakes. The tectonic zone to the north of the Main Boundary Fault is a highly fractured rock mass that may not accumulate strain in large enough volumes to give rise to great earthquakes. Although large earthquakes ($7 < M < 8$) have occurred there, none larger than $M = 8$ have been reported. For these reasons, in source zone 12 we identify the Main Boundary Fault as the major fault.

Major faults in source zone 10 encompassing the Shillong massif and the Bramhaputra valley in the northeastern region consist of those which have been identified on the Tectonic Map of India (Eremenko and Negi, 1968). These include the Dauki fault, the Haflong fracture zone and the Naga thrust. Over the Shillong massif three additional fault traces were drawn parallel to the Dauki fault to simulate the high seismic hazard over the entire massif. The great 1897 Assam earthquake caused extreme intensities in the entire area of the massif, termed the epicentral zone by Oldham (1899).

The hinge zone in source zone 11 is assumed to be a major fault since such features are associated with crustal movements. Major faults in source zones 2 and 5 are assumed to be on the Panvel flexure and the Narmada fault. A set of east-trend-

ing faults is postulated as major faults in source zone 3. Northeast-trending basement faults were assumed to be major faults in source zone 21. Major faults in source zone 16, 18, 19, and 24 were identified from the Geological Map of Asia and Far East (UNESCO, 1971), which also includes the Chaman fault. In the remaining source zones, major faults were not identified.

CALCULATION OF SEISMIC HAZARD

A series of master curves has been prepared by Perkins (1978) that is useful in making rapid preliminary estimates of expected peak accelerations due to point sources within source zones. These curves were used to estimate seismic hazard over large areas of the map. Detailed calculations of the seismic hazard were confined to eleven critical test areas (Fig. 10) that were selected to determine the effects of line-source seismicity, adjacent source zones and intermediate-depth earthquakes. The contours in the regions lying between the test areas were drawn on the basis of the contours in the adjacent areas and estimates obtained from the master curves. This procedure assumes that unless there is a perturbation in the seismicity rate, tectonic setting (e.g., in fault trends or major faults), or presence of new source zones, the trend of the contours could be extrapolated into regions adjacent to test areas. This procedure provides a fairly reliable description of all the source zones except in the western part of source zone 19. In this area, the tectonic architecture is quite complicated and the contours presented in the map are roughly generalized. Similarly, in source zones 1, 5, and 23 no attempt has been made to estimate peak accelerations in any detailed sense and average estimates were obtained using the master curves.

SEISMIC HAZARD MAP

The seismic hazard map for the Indian subcontinent prepared using actual hazard calculations and the master curves as described above, is shown in Fig. 11. The exposure period for this map is 50 years, and the peak accelerations represented on the map have a return period of 475 years. The probability of exceedance of these accelerations in 50 years is 10%. Continuous contours are drawn in those areas where detailed computer calculations were made. Where master curves were used, the contours are broken.

The seismic hazard map shows that the Indian shield is characterized by peak acceleration values of less than 5% g. Portions of the western coastal areas show higher expected peak acceleration of about 10% g near Bombay and 40% g in an area farther to the northwest. The seismotectonic provinces consisting of the Sulaiman, Karakoram, and Himalaya mountain belts bordering the shield in the northwest, north, and east have a high seismic hazard that is in conformity with high seismicity in those areas; the maximum value of estimated peak acceleration is about 70% g in

TABLE 2

The relative rate at which 10% g peak acceleration is exceeded for a mapped peak acceleration level

Mapped peak acceleration in percent g	Relative rate at which 10% g acceleration is exceeded	10% g return period (years)
5	0.4	1250
10	1.0	500
20	3.1	160
40	13.1	37
60	48	10
70	128	4

the Himalaya (source zone 12). The highest estimated peak acceleration value of (80% g) is obtained in the areas of the Bramhaputra valley (source zone 10) and the Quetta region (source zone 18) in the northwestern part of the Indian subcontinent. This belt of high seismic hazard continues southward enclosing the Andaman–Nicobar Islands. The maximum peak acceleration in the island areas, however, drops to about 45% g.

The Sindhu Ganga plains are characterized by an average of about 10% g peak acceleration values. The border between the plains and the mountains indicates values of about 20% g. The average peak acceleration in the Tibet area is estimated, using the master curves, to be of the order of 20% g.

If the relative rate of exceedance of 10% g peak acceleration at a 10% g contour is assumed to be one, then the relative rates of exceedance of 10% g in areas of other mapped peak acceleration levels are given in Table 2. Using this table, the expected frequency of exceedance of 10% g peak acceleration (the threshold of damage) can be estimated for any area.

The seismic hazard map (Case A) presented here is significantly influenced by the presence of major faults to which were assigned all earthquakes with $M > 7.5$. in zones where such faults were used. A seismic hazard map (Case B) could have been prepared by distributing all the seismicity on regularly spaced fault lines representing the tectonic lineament of the source zone. Case A would reflect higher peak accelerations in the vicinity of a major fault zone compared to Case B, while away from a major fault zone, Case A would reflect lower peak accelerations than Case B. For example, in source zone 10, near the Dauki fault, Case A accelerations are about 70% g, while Case B accelerations are about 45–50% g. Away from this fault, accelerations are 30–40% g for Case A, while Case B is unchanged.

The hazard estimates in source zones of peninsular India may have lower reliability relative to other zones due to a lack of well established earthquake occurrence rates. This problem may only be resolved by future detailed seismic monitoring and improved understanding of the neo-tectonics of this region.

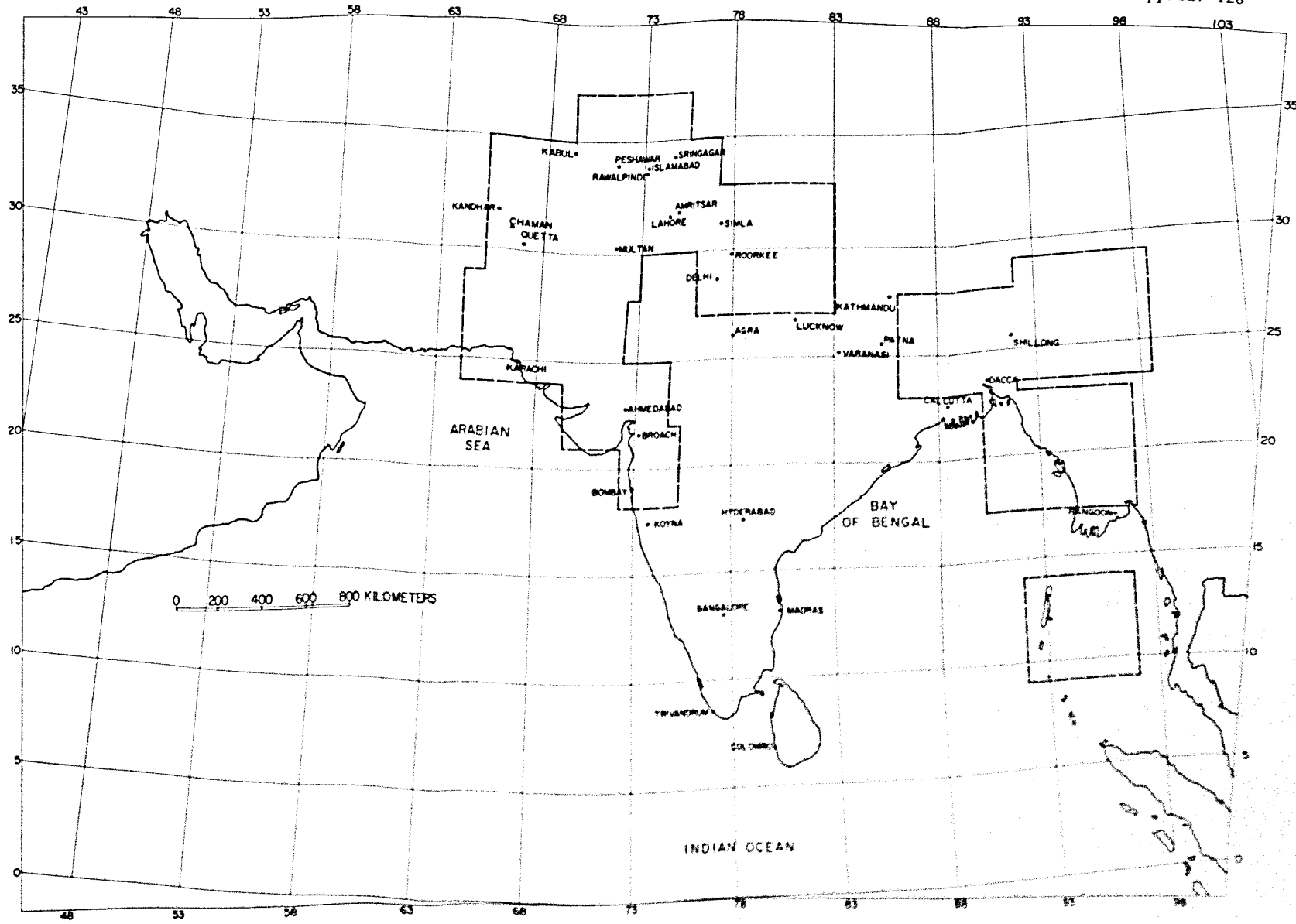

Fig. 10. Test regions over which detailed computation of the seismic hazards were conducted.

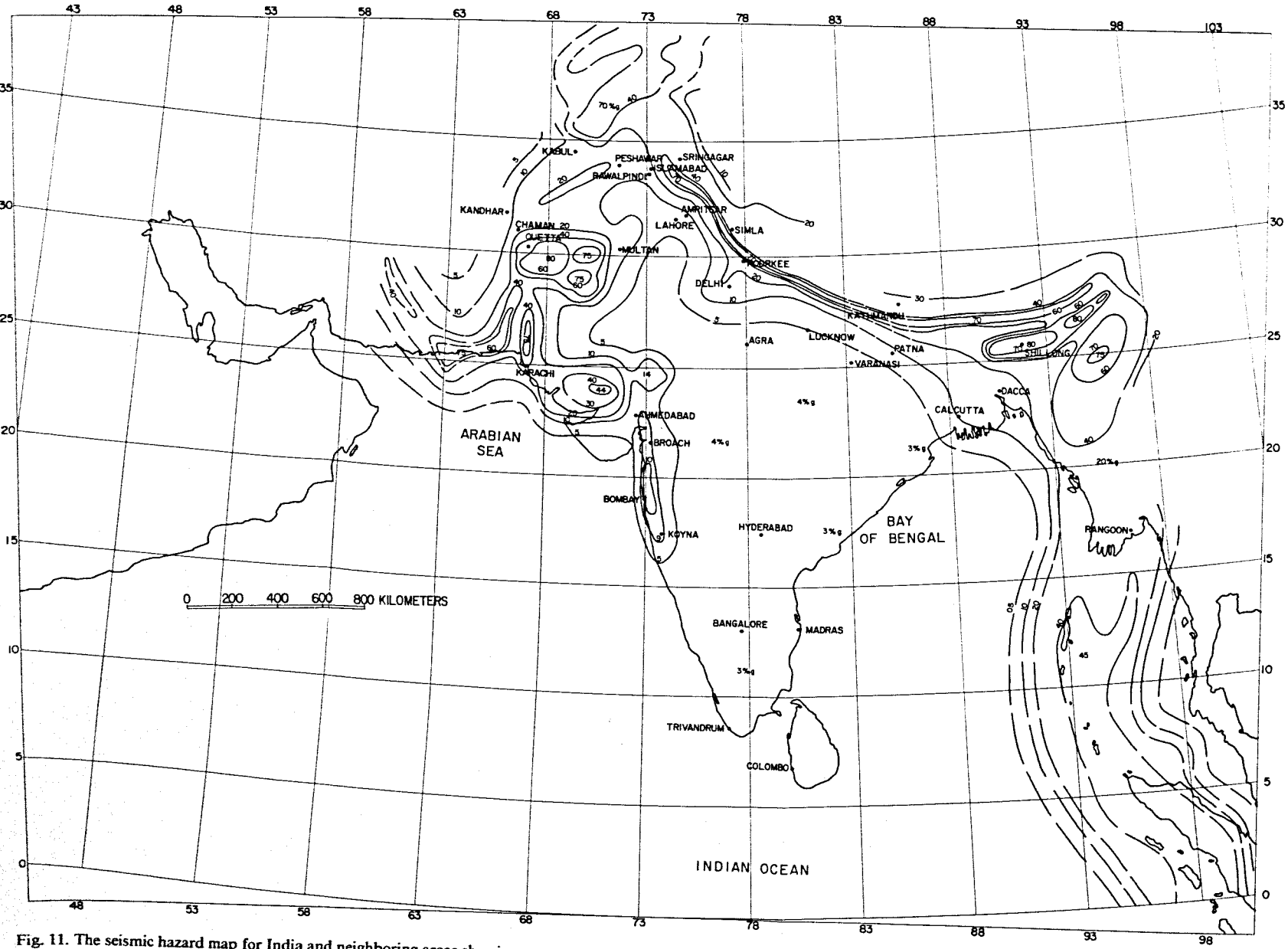

Fig. 11. The seismic hazard map for India and neighboring areas showing contours of expected peak accelerations in rock in percent *g*. The exposure period for this map is 50 years. The probability of exceedence of the mapped accelerations in 50 years in 10%. The return period of the peak acceleraions is 475 years.

The uncertainty in the attenuation-distance law may also impose limitations on the precision of the hazard map. The departures of actual behavior from the relationships used here in the very near as well as in the far field regions may not be significant for peak acceleration values having a return period of 475 years (Algermissen et al., 1982). The map is expected to preserve the proper contrast in hazard, although the absolute level is not firmly established in the absence of instrumental records of strong earthquake motion in this region.

The intermediate-depth earthquakes, as modeled here, did not contribute significantly to the seismic hazard except in source zones 9 and 24. The main reasons for this seem to be the significantly lower seismic rates, as well as, lower expected maximum magnitudes in the intermediate depth zone compared to those for shallow focus seismicity. Furthermore the larger hypocentral distances for intermediate-depth earthquakes reduced their effect compared to that of shallow-focus earthquakes.

Comparison of this map with those of Basu and Nigam (1977, 1978) show values of peak accelerations that are lower than ours by factors of 1.5–2 where peak accelerations are high, e.g., in the Himalaya seismotectonic region. This difference is probably due to our use of a line source model, which significantly reduces the return period of high accelerations, compared to their source model.

Finally, it should be noted that the seismic hazard map presents the average value of expected peak acceleration in rock. The effect of local site conditions should be accounted for by choosing a suitable site amplification factor to modify the peak acceleration presented in this map. The peak acceleration values shown in the map can serve as an objective basis for scaling of the design earthquake spectrum.

ACKNOWLEDGEMENTS

We wish to acknowledge the thoughtful and helpful comments W. Spence, J. Dewey, and F. McKeown gave us on the initial manuscript. Portions of this study were performed while the first author was a visiting fellow at CIRES at the University of Colorado, Boulder, Colorado, and were partially funded by the U.S. Geological Survey. The University of Roorkee kindly granted the first author leave to pursue this investigation.

REFERENCES

Algermissen, S.T. and Perkins, D.M., 1976. A probabilistic estimate of maximum acceleration in rock in the contiguous United States. U.S. Geol. Surv. Open-File Rep., 76-416, 45 pp.

Algermissen, S.T., Perkins, D.M., Thenhaus, P.C., Hanson, S.L. and Bender, B.L., 1982. Probabilistic estimates of maximum acceleration and velocity in rock in the contiguous United States. U.S. Geol. Surv., Open-File Rep., 82-1033, 99 pp.

Auden, J.B., 1959. Earthquakes in relation to the Damodar Valley Project. Proc. Symp. Earthquake Eng., 1st, Univ. Roorkee, Roorkee.

Auden, J.B., 1969. Geological report on the seismicity of parts of western India, including Maharashtra. Unesco Rep., Ser. No. 1519/BMS.RD/SCE, Paris, 38 pp.

Auden, J.B. and Ghosh, A.M.N., 1934. Preliminary account of the earthquake of the 15th January, 1934, in Bihar and Nepal. Rec. Geol. Surv. India, 68(2): 177–239.

Avasthi, D.N., Varadarajan, S. and Rao, N.D.J. 1971. Study of the Deccan trap of the Cambay basin by geophysical methods. Bull. Volcanol., 35(3): 743–749.

Basu, S. and Nigam, N.C., 1977. Seismic risk analysis of Indian Peninsula. Proc. World Conf. Earthquake Eng., 6th, New Delhi, 2: 425–431.

Basu, S. and Nigam, N.C., 1978. On seismic zoning map of India. Proc. Symp. Earthquake Eng., 4th Univ. Roorkee, Roorkee, 1: 83–90.

Basu, S. and Srivastava, L.S., 1981. Seismic design zoning map of India. Symp. Earthquake Disaster Mitigation, Univ. Roorkee, Roorkee, 1: 99–109.

Båth, M., 1975. Seismicity of the Tanzania region. Tectonophysics, 27: 353–379.

Båth, M., 1977. Teleseismic magnitude relations. Ann. Geofis., 17: 315–398.

Båth, M., 1978. A note on recurrence relations for earthquakes. Tectonophysics, 51: T23–T30.

Båth, M., 1981. Earthquake recurrence of a particular type. Pure Appl. Geophys., 119: 1063–1076.

Ben Menahem, A, Aboodi, E. and Schild, R., 1974. The source of the great Assam earthquake—an interplate wedge motion. Phys. Earth Planet. Inter., 9: 265–289.

Bonilla, M.G. and Buchnan, J.M., 1970. Interim report on world wide historic faulting. U.S. Geol. Surv., Open-File Rep., 32 pp.

Bune, V.I., Vedenskaya, N.A. and Gzovskij, M.V., 1976. The methodological fundamentals of large-scale seismic zoning. In: S.V. Medvedev (Editor), Seismic Zoning of the USSR. Israel Program for Scientific Translations, Jerusalem, p. 533.

Burke, K. and Dewey, J.F., 1973. Plume generated triple junctions: key indicators in applying plate tectonics to old rocks. J. Geol., 81: 406–433.

Chandra, U., 1977. Earthquakes of peninsular India–a seismotectonic study. Bull. Seismol. Soc. Am., 67: 1387–1414.

Chandra, U., 1978. Seismicity, earthquake mechanisms and tectonics along the Himalayan mountain range and vicinity. Phys. Earth Planet. Inter., 16: 109–131.

Cornell, C.A., 1968. Engineering seismic risk analysis. Bull. Seismol. Soc. Am., 58: 1583–1606.

Deshikachar, S.V., 1974. A review of the tectonic and geological history of eastern India in terms of "plate tectonics" theory. J. Geol. Soc. India, 15: 137–149.

Eremenko, N.A. and Negi, B.S., 1968. A guide to the tectonic map of India. Oil and Natural Gas Commission, India, pp. 1–15.

Evans, P., 1964. The tectonic framework of Assam. J. Geol. Soc. India, 5: 80–96.

Fitch, T.J., 1970. Earthquake mechanisms and island arc tectonics in the Indonesian–Philippine region. Bull. Seismol. Soc. Am., 60: 565–592.

Fitch, T.J., 1972. Plate convergence, transcurrent faults, and internal deformation adjacent to southeast Asia and the Western Pacific. J. Geophys. Res., 77: 4432–4460.

Gansser, A., 1964. Geology of the Himalayas. Interscience, New York, 289 pp.

Gaur, V.K. and Chouhan, R.K.S., 1968. Quantitative measures of seismicity applied to Indian regions. Bull. Indian Soc. Earthquake Technol., 5: 63–78.

Gee, E.R., 1934. The Dhubri earthquake of the 3rd July, 1930. Mem. Geol. Surv. India, 65(1): 1–106.

Geological Survey of India, 1974. Geology and mineral resources of the states of India. IV. Arunachal Pradesh, Assam, Manipur, Meghalaya, Mizoram, Nagaland and Tripura. Geol. Surv. India, Misc. Publ., 30: 124 pp.

Geological Survey of India, 1979. Geology of Himalaya, Appraisal of status and definition of problems. Himalayan Geol. Sem., New Delhi, 1976. Sect. I: Geol., Stratigr. Paleontol.—Geol. Surv. India, Misc. Publ., 41: 1–48.

Goshkov, G.P., 1974. Seismotectonic relations (Geologic criteria of earthquake origins). Proc. of the Seminar on the Seismotectonic Map of the Balkan Region—UNESCO, pp. 239–259.

Gosavi, P.D., Bapat, A.V. and Guha, S.K., 1977. Macroseismic studies of four recent Indian earthquakes. Proc. World Conf. Earthquake Eng., 6th New Delhi, 1: 49–54.

Gubin, I.E., 1968. Seismic zoning of Indian peninsula. Bull. Int. Inst. Seismol. Earthquake Eng., 5: 109–139.

Guha, S.K., 1962. Seismic regionalization of India. Proc. Symp. Earthquake Eng., 2nd, Roorkee, pp. 191–207.

Gupta, H.K., Narain, H., Rastogi, B.K. and Mohan, I., 1969. A study of the Koyna earthquake of December 10, 1967. Bull Seismol. Soc. Am., 59: 1149–1162.

Gupta, H.K., Mohan, I. and Narain, H., 1972. The Broach earthquake of March 23, 1970. Bull. Seismol. Soc. Am., 62: 47–61.

Gutenberg, B. and Richter, C.F., 1956. Earthquake magnitude, intensity, energy, and acceleration. Bull. Seismol. Soc. Am., 46; 105–145.

Gutenberg, B. and Richter, C.F., 1965. Seismicity of the Earth and Associated Phenomena. Hafner, New York, 310 pp.

Hattori, S., 1979. Seismic risk maps in the world (maximum acceleration and maximum particle velocity). II. Balkan, Middle East, South East Asia, Central America, South America and others. Bull. Int. Inst. Seismol. Earthquake Eng., 17: 33–96.

Herrmann, R.B., 1977. Recurrence relations. Earthquake Notes, 48: 47–49.

Housner, G.W., 1965. Intensity of earthquake ground shaking near the causative fault. Proc. World Conf. Earthquake Eng., 3rd, 1: III 94–III 115.

Howell, B.F. and Schultz, T.R., 1975. Attenuation of modified Mercalli intensity with distance from the epicenter. Bull Seismol. Soc. Am., 65: 651–665.

Ichikawa, M., Srivastava, H.N., Drakopoulos, J., 1972. Focal mechanisms of earthquake occurring in and around the Himalayan and Burmese Mountain belts. Pap. Meteorol. Geophys. (Tokyo), 23: 149–162.

I.S.I., 1975. Indian standard recommendations for earthquake resistant design of structures. Indian Standards Institution, New Delhi, 15: 1893–1975.

Kaila, K.L. and Rao, M., 1979. Seismic zoning maps of the Indian subcontinent. Geophys. Res. Bull., 17(4): 293–301.

Kaila, K.L., Gaur, V.K. and Narain, H., 1972. Quantitative seismicity maps of India. Bull. Seismol. Soc. Am., 62: 1119–1132.

Khattri, K., Rogers, A.M. and Perkins, D.M., 1978. Seismic risk map of the Koyna–Bombay–Ahmedabad area, India. Proc. Symp. Earthquake Eng., 6th, Roorkee, I: 91–96.

Krishna, J., 1959. Seismic zoning of India. Proc. Symp. Earthquake Eng., 1st, Univ. Roorkee, Roorkee.

Krishnan, M.S., 1953. The structural and tectonic history of India. Mem. Geol. Surv. India, 81: 1–137.

Krishnan, M.S., 1968. Geology of India and Burma. Higginbothams, Madras, 536 pp.

LeFort, P., 1975. Himalayas: the collided range. Present knowledge of the continental arc. Am. J. Sci., 275-A: 1–44.

Mathur, L.P., Rao, K.L.N. Chaube, A.N., 1968. Tectonic framework of Cambay basin India. Oil Nat. Gas Comm. Bull., 5(1): 7–28.

McCann, W.R., Nishenko, S.P., Sykes, L.R. and Krause, J., 1979. Seismic gaps and plate tectonics: seismic potential for major plate boundaries. Pure Appl. Geophys., 117 (6): 1082.

McConnell, R.B., 1974. Evolution of taphrogenic lineaments in continental platforms. Geol. Rundsch., 63(2): 389–430.

Medvedev, S.V., 1959. Correlation between focal depth of earthquakes and isoseismals. In: Problems in Engineering Seismology, Vol. 2. Tr. Inst. Fiz. Zemli, Akad. Nauk. SSSR, 5 (172): 94–99 (in Russian).

Middlemiss, C.S., 1910. The Kangra earthquake of 4th April 1905. Mem. Geol. Surv. India, 38: 409 pp.

Mithal, R.S. and Srivastava, L.S., 1959. Geotectonic position and earthquakes of Gango–Bramhaputra region. Proc. Symp. Earthquake Eng., 1st, Univ. Roorkee, Roorkee.

Molnar, P., Fitch, T.S., Wu, F.T., 1973. Fault plane solutions of shallow earthquakes and contemporary tectonics in Asia. Earth Planet. Sci. Lett., 19: 101–112.

Murthy, M., Talukdar, S.C. and Bhattacharya, A.C., 1969. The Dajki fault of Assam, India. Oil Nat. Gas Comm. Bull., G(2): 57–64.

Naqvi, S.M. Rao, V.D. and Narian, H., 1974. The protocontinental growth of the Indian shield and the antiquity of its rift valleys. Precambrian Res., 1: 345–398.

Neumann, F., 1954. Earthquake Intensity and Related Ground Motion. Washington Univ. Press, Seattle, Wash., 77 pp.

Oldham, R.D., 1883. Catalogue of India earthquakes. Mem. Geol. Surv. India, 19: 163–215.

Oldham, R.D., 1889. Report of the great earthquake of 12th June 1897. Mem. Geol. Surv. India, 29: 1–379.

Oldham, R.D., 1926. The Cutch earthquake of 16th June, 1819, with a revision of the Great (Assam) earthquake of 12th June, 1897. Mem. Geol. Surv. India, 46(2): 1–77.

Perkins, D.M., 1978. Acceleration hazard map sensitivity to input seismic parameters. Boll. Geofis, Teor. Appl., 20: 188–196.

Raju, A.T.R., 1968. Geological evolution of Assam and Cambay Tertiary basins of India. Bull. Am. Assoc. Pet. Geol., 52: 2422–2437.

Richter, C.F., 1958. Elementary Seismology. Freeman, San Francisco, Calif., 768 pp.

Sengupta, S., 1966. Geological and geophysical studies in the western part of Bengal Basin, India. Bull. Am. Assoc. Pet. Geol., 50: 1001–1017.

Sengupta, S.N. and Khattri, K.N., 1975. Some aspects of geodynamics of Indian sub-continent. Proc. Indian Natl. Sci. Acad., 41, pt. A, (4): 339–357.

Singh, S., Jain, A.K., Sinha, P., Singh, V.N. and Srivastava, L.S., 1976. The Kinnaur earthquake of January 19, 1975: a field report. Bull. Seismol. Soc. Am., 66: 887–901.

Sinvhal, H., Singh, V.N., Mithal, D.K. Khattri, K.N. and Gaur, V.K., 1976. Seismic zoning of the Utlar Pradesh for engineering purposes. Symp. on Contribution of Earth Sciences towards Research and Developmental Activities in the Northern Region, India. Geol. Surv. India.

Sinvhal, H., Khattri, K.N., Rai, K. and Gaur, V.K., 1978. Neotectonics and time-space seismicity of the Andaman–Nicobar region. Bull. Seismol. Soc. Am. 68: 399–409.

Srivastava, L.S., 1976. Seismic zoning of India. In: A.S. Arya et al. (Editors), Earthquake Engineering. Sariska Prakashan, Meerut, pp. 49–65.

Stauder, W., 1968. Tensional character of earthquake foci beneath the Aleutian trench with relation to sea-floor spreading. J. Geophys. Res., 73: 7693–7701.

Stepp, J.C., 1973. Analysis of completeness of the earthquake sample in the Puget Sound area. In: S.T. Harding (Editor), Contributions to Seismic Zoning. NOAA TEch. Rep., ERL 267–ESL 30, U.S. Dep Commerce.

Stuart, M., 1920. The Srimangal earthquake of 8th July 1918. Mem. Geol. Surv. India, 46(1): 1–70.

Tandon, A.N., 1950. The very great earthquake of August 15, 1950. Sci. Cult., 147–155.

Tandon, A.N., 1956. Zones of India liable to earthquake damage. Ind. J. Meteorol. Geophys., 10: 137–146.

UNESCO, 1971. Geological map of Asia and the Far East. Scale 1:5,000,000. U.N. Publ. No. 69-30632—UNESCO, Paris.

Valdiya, K.S., 1973. Tectonic framework of India: a review and interpretation of recent structural and tectonic studies. Geophys. Res. Bull., 11: 79–114.

Verma, R.K., Mukhopadhyay, M. and Ahluvalia, M.S., 1976. Earthquake mechanisms and tectonic features of northern Burma. Tectonophysics, 32: 387–399.

Wadia, D.N., 1957. Geology of India. Macmillan, London, 3rd ed., 536 pp.

West, W.D., 1937. Earthquakes in India (presidential address). Ind. Sci. Congr., 24th, Hyderabad, Proc., pp. 189–227.